IV International Conference on Particle-based Methods – Fundamentals and Applications
PARTICLES 2015
E. Oñate, M. Bischoff, D.R.J. Owen, P. Wriggers & T. Zohdi (Eds)

USING DELAUNAY TRIANGULATIONS TO INVESTIGATE THE EFFECT OF INTERPARTICLE FRICTION ON CRITICAL-STATE DEM SIMULATIONS

KEVIN J. HANLEY[1], XIN HUANG[2] AND CATHERINE O'SULLIVAN[3]

[1] Institute for Infrastructure and Environment, School of Engineering,
The University of Edinburgh, Edinburgh EH9 3JL, UK
k.hanley@ed.ac.uk

[2] Department of Geotechnical Engineering, School of Civil Engineering
& Key Laboratory of Geotechnical Engineering,
Tongji University, Shanghai 200092, China
xhuang@tongji.edu.cn

[3] Department of Civil and Environmental Engineering,
Imperial College London, London SW7 2AZ, UK
cath.osullivan@imperial.ac.uk

Key words: Critical-state soil mechanics, Triaxial shearing, Contact network, Strong force chains, Delaunay triangulation.

Summary. *It is now broadly accepted that failure in a granular material is dominated by buckling failure of strong force chains oriented in the direction of the major principal stress. In this paper, Delaunay triangulation is used to explore the role of the interparticle friction coefficient (μ) in stabilising these strong force chains. An isotropic numerical sample was created in 3D which contains 20,164 polydisperse spherical particles inside a periodic cell. μ was changed to 0.0, 0.1, 0.25, 0.5, 0.75 or 1.0 to create six samples, each of which was sheared triaxially until critical state was attained. The contact network was obtained at the end of each simulation by joining the centroids of the contacting particles. The Voro++ software library was used to compute two types of periodic Voronoi tessellation of the particle centroids: the conventional unweighted tessellation and the radical tessellation which is weighted by particle diameter. These were converted to their Delaunay duals to facilitate direct comparison with the associated contact networks. The numbers of edges (i.e., contacts) that are in the contact networks decrease consistently as μ is increased towards 1. This contrasts with the numbers of edges, faces or tetrahedra in the Delaunay triangulations, all of which increase with increasing μ up to μ = 0.25 and become approximately constant thereafter. Two quantities were defined: the percentage of faces in the triangulation comprising three contacts (P_{fc}) and the percentage of tetrahedra comprising six contacts (P_{tc}). P_{fc} shows a linearly-decreasing trend with increasing angle of shearing resistance and both P_{fc} and P_{tc} decrease continuously as μ is increased. This indicates that triangular motifs become less widespread as friction increases and that the weak supporting network which is present at low μ values is effectively absent at high μ.*

1 INTRODUCTION

The stress distribution within any granular material subjected to load is highly heterogeneous. Strong force chains, consisting of contacting particles aligned with the major principal stress orientation, form upon loading to transmit the majority of the load and carry the deviatoric stress during shear deformation. These strong force chains are supported by a weak orthogonal contact network. The formation of strong force chains has been observed experimentally using image analysis [1], tomography [2] and photoelasticity [3]. The development of strong force chains supported by a weak orthogonal network has often been observed in discrete element method (DEM) simulations, e.g., [4-6]. Over the last 15 years, it has become increasingly widely accepted that the dominant failure mechanism in a granular material is buckling failure of the strong force chains. Evidence supporting this hypothesis has been provided by a range of complementary investigation tools such as DEM simulation [7], photoelasticity experiments [8] and analytical modelling [9-11].

A parametric study was conducted recently [12] in which three-dimensional numerical samples were sheared triaxially to a critical state using different values of the interparticle friction coefficient (μ). This was an extension of previous DEM studies on the same subject [13,14]. It was found that the stability of the strong force chains increases with increasing μ while the supporting weak contact network has greatest importance for stabilising the strong force chains at low values of μ [12]. In this paper, the same data set is analysed using Delaunay triangulation of the particle centroids. The principal aim of this short study is to investigate whether triangular motifs become less common and linear structures more so as μ is increased: [15] found this to be the case for two-dimensional packings of disks but this finding has not been observed in 3D, to the best of the authors' knowledge.

2 DEM SIMULATIONS

A 3D numerical sample was created by randomly placing 20,164 polydisperse spherical particles within a periodic cell. These boundary conditions were chosen to avoid inhomogeneities at the periphery of the sample [16]. The periodic cell was initially cubical, consisting of three pairs of mutually-orthogonal periodic boundaries. The particle size distribution of the numerical sample, shown in Figure 1, is representative of Toyoura sand with a ratio of maximum to minimum particle diameters of around 3.6. A simplified Hertz-Mindlin contact model was used. The particle shear modulus and Poisson's ratio were set at 29 GPa and 0.12, respectively, to match experimentally-measured properties of quartz [17]. The particle density was set at 2650 kg/m^3: a realistic value for a quartz sand. Gravity was inactive throughout the simulations. A stable isotropic assembly was created at a confining pressure of 100 kPa by moving opposing pairs of periodic boundaries closer together using a stress-control algorithm. The interparticle friction coefficient was 0.0 at this stage. Following isotropic compression, the interparticle friction coefficient was changed to 0.0, 0.1, 0.25, 0.5, 0.75 or 1.0. Each of these six samples was subjected to drained triaxial shearing to an axial strain of around 54%. This strain level was sufficient to reach the critical state in all simulations. All of these simulations were run using a version of the open-source LAMMPS code [18] which has been modified by the authors to include a stress-control algorithm for periodically-bounded samples and contact models which have been revised substantially to correspond to those in [19,20].

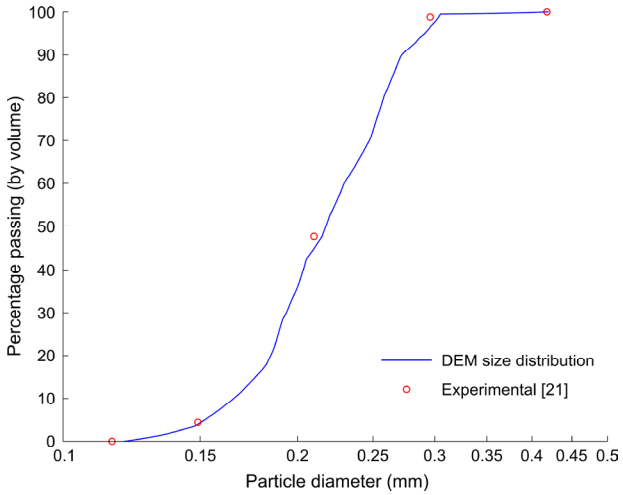

Figure 1: Particle size distribution of the numerical simple compared with a digitised size distribution of a real Toyoura sand measured by sieve analysis [21]

3 DATA ANALYSIS

The six samples were compared only at the end of the triaxial simulations, at around 54% axial strain, once critical state had been attained. Critical state is characterised by the continued deformation of a sample under shear without a change in either volume or stress state. The contact networks were easily obtained by joining the centroids of the contacting particles. Each interparticle contact corresponds to an edge in the contact network. In addition, Voronoi tessellations were computed based on the particle centroids. Voro++ [22] was chosen for this analysis as it is capable of doing periodic tessellations with non-cubical cells. In these simulations, the samples are almost cubical at the end of isotropic compression but become highly non-cubical during shearing. Two types of periodic Voronoi tessellation were computed: the conventional unweighted tessellation which does not take particle diameter into account and the radical (or Laguerre) tessellation which is weighted by particle diameter. These were converted to their Delaunay duals using MATLAB [23]. This conversion facilitated a direct comparison between the edges of the Delaunay tessellations and the edges of the associated contact networks.

4 RESULTS AND DISCUSSION

Figures showing the macro-scale response of five of the six samples (excluding the frictionless simulation) are provided in [12]. Table 1 summarises the key macro-scale results at the critical state of each simulation. In Table 1, φ'_{cv} is the angle of shearing resistance and e is the void ratio, defined according to the soil mechanics convention as the volume of voids divided by the volume of solids. $q = \sigma'_1 - \sigma'_3$ is the deviatoric stress and $p' = \frac{\sigma'_1 + 2\sigma'_3}{3}$ is the mean effective stress where σ'_1, σ'_2 and σ'_3 represent the major, intermediate and minor principal effective stresses, respectively. $\sigma'_2 = \sigma'_3$ for these axisymmetric triaxial simulations.

Table 1: Macro-scale data at the end of the six simulations after the attainment of critical state

μ	q (kPa)	p' (kPa)	φ'_{cv} (°)	e
0.0	23.951	107.99	4.98	0.5344
0.1	61.885	120.63	13.54	0.5909
0.25	87.794	129.27	18.17	0.6317
0.5	99.514	133.18	19.97	0.6504
0.75	90.418	130.14	20.19	0.6527
1.0	100.49	133.50	20.98	0.6542

The number of particles is constant throughout these simulations; therefore, the coordination number is directly proportional to the number of edges in a contact network. Figure 2 shows that the number of edges (or equivalently the coordination number) decreases with increasing μ from around 57,000 at μ = 0.0 to 32,000 when μ = 1.0. The opposite trend is observed in the void ratio which increases with increasing μ as shown on the secondary vertical axis on Figure 2. As μ decreases, particles are packed together more closely and so a corresponding increase in the number of contacts is unsurprising.

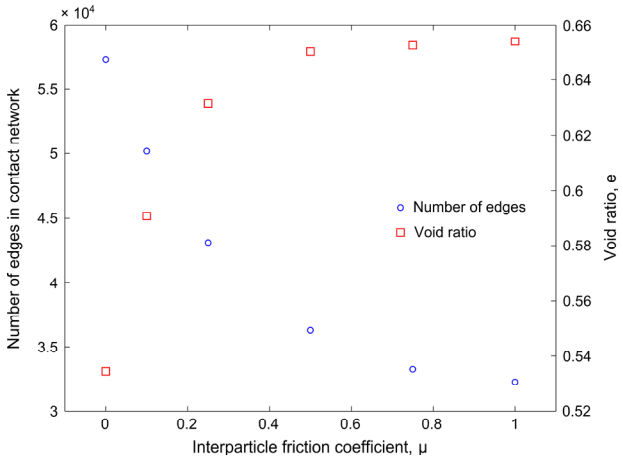

Figure 2: The variations in the number of contacts and the void ratio at the critical state with the interparticle friction coefficient

Although the number of contacts decreases with increasing μ, Figure 3 shows the opposite trend for the number of edges in the Delaunay triangulations which increases with μ up to μ = 0.25 and remains approximately constant thereafter. This is the case for both the conventional, unweighted tessellation based solely on the particle centroids and for the radical tessellation which is weighted by particle diameter.

The numbers of faces or tetrahedra in the Delaunay triangulations also increase with increasing μ up to μ = 0.25 as shown in Figures 4 and 5. Further increases in μ beyond 0.25 do not affect the numbers of faces or tetrahedra in the triangulations. This is perhaps expected from Figure 3 as each face comprises three edges and each tetrahedron comprises six edges. The existence of a threshold beyond which the system shows little sensitivity to μ is reported by [12] who found that the critical-state loci were almost identical for μ = 0.5, 0.75 and 1.0. However, [12] observed substantial differences between μ = 0.25 and μ = 0.5, exemplified by

the differences in void ratio in Table 1. Based on Figures 3-5, it seems that triangulations of the particle centroids 'saturate' at lower values of μ than conventional macro-scale measures such as q, p' or e.

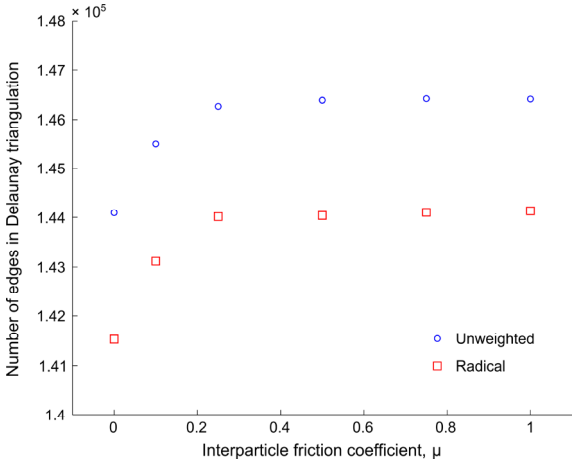

Figure 3: The number of edges in the Delaunay triangulations against the interparticle friction coefficient at the critical state

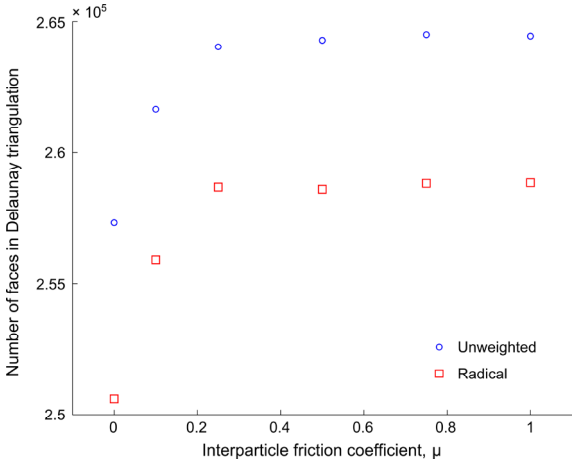

Figure 4: The number of faces in the Delaunay triangulations against the interparticle friction coefficient at the critical state

Two distinct sets of edges connecting particle centroids are available for each simulation: one set of interparticle contacts and one set of Delaunay triangulation edges. These may be compared as some edges are common to, or absent from, both sets, while some edges appear only in the Delaunay set. Every single interparticle contact is present among the associated Delaunay triangulation edges; hence the interparticle contacts may be regarded as a subset of the Delaunay triangulation edges. By comparing Figures 2 and 3, it is apparent that there are between 2.4 and 4.6 times more edges in any Delaunay triangulation than there are in the corresponding contact network. Figure 6 shows the percentage of triangulation edges which are contacts for each simulation. These results are very similar for both types of Voronoi tessellation. As the number of contacts decreases with increasing μ and the number of

Delaunay edges increases with increasing μ, Figure 6 exhibits a sharp decrease as μ increases.

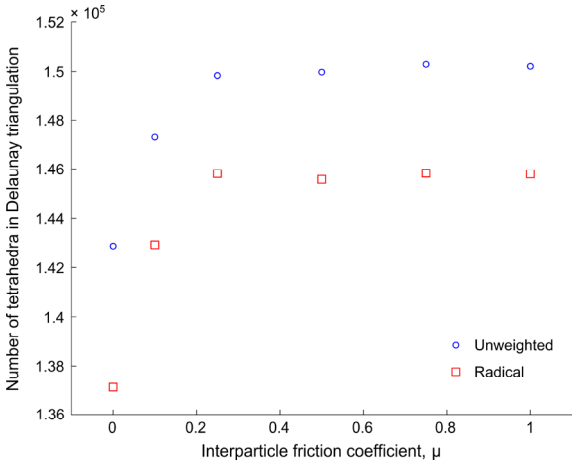

Figure 5: The number of tetrahedra in the Delaunay triangulations against the interparticle friction coefficient at the critical state

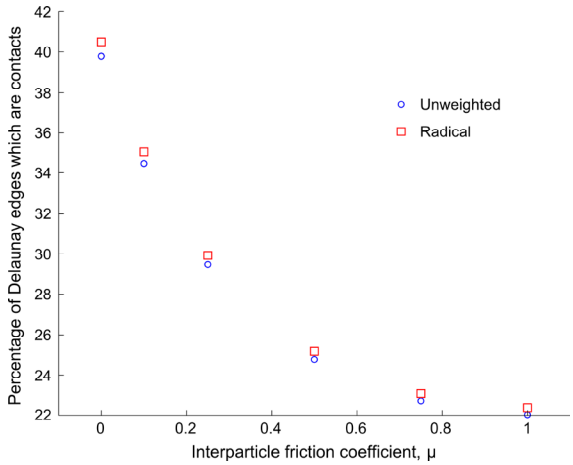

Figure 6: The percentage of Delaunay triangulation edges which are interparticle contacts for each simulation against the interparticle friction coefficient

Two quantities were defined: the percentage of faces in the triangulation comprising three interparticle contacts (P_{fc}) and the percentage of tetrahedra comprising six contacts (P_{tc}). P_{fc} and P_{tc} are respectively plotted against the interparticle friction coefficient on Figures 7 and 8. Both P_{fc} and P_{tc} decrease monotonically as μ is increased. These two figures support the hypothesis of Smart and Ottino [15] that triangular motifs become less widespread as friction increases. Furthermore, these figures also provide additional evidence for the observation that a weak supporting network develops during shearing only at low μ values [12]: the support provided to a strong force chain by weak contacts necessarily creates many triangular arrangements of particles which are far less prevalent at high μ than at low μ values.

Many DEM simulations have shown that there is a non-linear relationship between the angle of shearing resistance, φ'_{cv}, and the interparticle friction coefficient, μ, or equivalently the interparticle friction angle, $\varphi'_p = \arctan \mu$ [7,12-14]. The reason for this non-linear

relationship remains the subject of some debate and is often poorly captured by analytical models [24-26]. One explanation is the interplay between rolling and sliding at the particle contacts [12]; this is not captured correctly by existing analytical models which neglect the effect of buckling. Prior research has shown that the critical buckling load has a non-linear relationship with μ and there exists a threshold value of μ beyond which the critical buckling load becomes invariant, as is the case for φ'_{cv} [12].

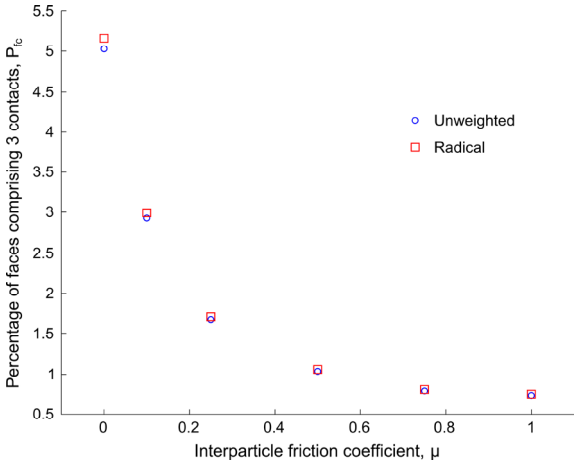

Figure 7: The percentage of Delaunay triangulation faces which are composed of three interparticle contacts against the interparticle friction coefficient at the critical state

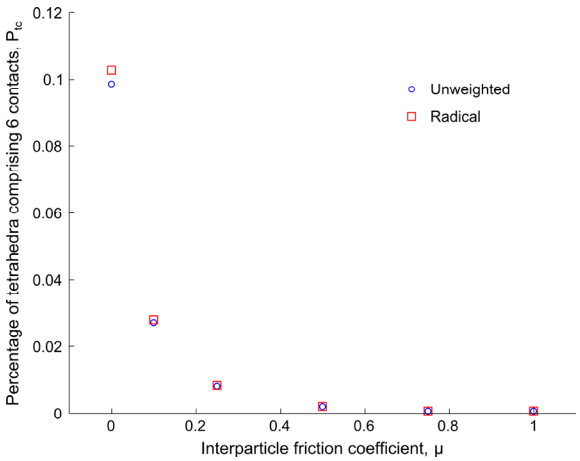

Figure 8: The percentage of Delaunay triangulation tetrahedra which are composed of six interparticle contacts against the interparticle friction coefficient at the critical state

Figure 9 shows that increasing μ reduces P_{fc} (Figure 7) but increases φ'_{cv}. The regressions on Figure 9 show that the relationship between P_{fc} and φ'_{cv} is almost linear. Interestingly, the shear resistance increases when the proportion of triangular structures is reduced. This is somewhat counter-intuitive: triangular structures tend to be more robust and tolerant to variations in the loading direction than columnar structures which are strong only when subjected to an axial load. It seems that the effect of μ on strength is much more significant than the proportion of triangular structures; having a relatively large proportion of triangular

structures at low μ does not noticeably affect φ'_{cv}. Another way of looking at these results is that the contribution to strength due to interparticle friction is dominant compared with the contribution to strength due to micro-scale particle geometry.

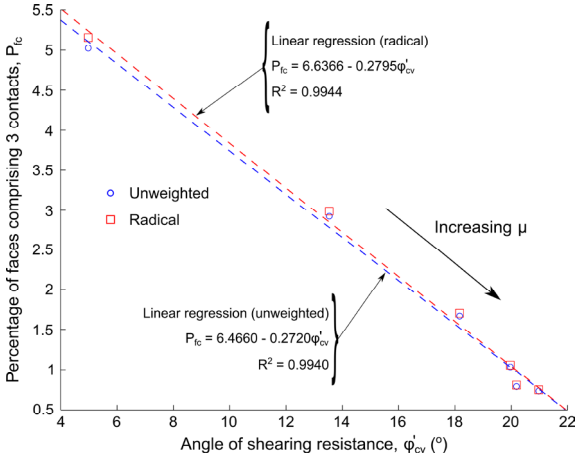

Figure 9: The percentage of Delaunay triangulation faces which are composed of three interparticle contacts against the angle of shearing resistance (°)

5 CONCLUSIONS

Six polydisperse numerical samples with differing interparticle friction coefficients were sheared triaxially to critical state. Contact networks were obtained and periodic Delaunay tessellations were computed at the end of each simulation using the particle centroids. The numbers of edges that are in the contact networks decrease consistently as μ is increased. This contrasts with the numbers of edges, faces or tetrahedra in the Delaunay triangulations, all of which increase with increasing μ up to μ = 0.25 and become approximately constant thereafter. The existence of a threshold beyond which the system shows little sensitivity to μ is also reported by [12]. Two quantities were defined, both of which decrease monotonically as μ is increased: the percentage of faces in the triangulation comprising three contacts (P_{fc}) and the percentage of tetrahedra comprising six contacts (P_{tc}). These results provide additional evidence for the observations that triangular motifs become less widespread as friction increases [15] and that a mechanically-stable, weak supporting network has greatest importance for stabilising the strong force chains at low values of μ [12]. P_{fc} shows a linearly-decreasing trend with increasing angle of shearing resistance, i.e., the shear resistance increases when the proportion of triangular structures is reduced. This implies that the effect of having a relatively large proportion of triangular structures at low μ is insignificant compared to the effect of μ on the rolling/sliding behaviour [12].

REFERENCES

[1] Rechemacher, A., Abedi, S. and Chupin, O. Evolution of force chains in shear bands in sands. *Géotechnique* (2010) **60**(5): 343-351.

[2] Hasan, A. and Alshibli, K.A. Experimental assessment of 3D particle-to-particle

interaction within sheared sand using synchrontron microtomography. *Géotechnique* (2010) **60**(5): 369-379.
[3] de Josselin de Jong, G. and Verrujit, A. Étude photo-élastique d'un empilement de disques. *Cah. Grpe fr. Etud. Rheol*. (1969) **2**: 73-86.
[4] Rothenburg, L. and Bathurst, R.J. Analytical study of induced anisotropy in idealized granular materials. *Géotechnique* (1989) **39**(4): 601-614.
[5] Barreto, D. and O'Sullivan, C. The influence of inter-particle friction and the intermediate stress ratio on soil response under generalised stress conditions. *Granul. Matter* (2012) **14**(4): 505-521.
[6] Radjai, F., Wolf, D.E., Jean, M. and Moreau, J.-J. Bimodal character of stress transmission in granular packings. *Phys. Rev. Lett.* (1998) **80**(1): 61-64.
[7] Thornton, C. Numerical simulations of deviatoric shear deformation of granular media. *Géotechnique* (2000) **50**(1): 43-53.
[8] Behringer, R.P., Daniels, K.E., Majmudar, T.S. and Sperl M. Fluctuations, correlations and transitions in granular materials: statistical mechanics for a non-conventional system. *Philos. Trans. A Math. Phys. Eng. Sci*. (2008) **366**: 493-504.
[9] O'Sullivan, C., Wadee, M.A., Hanley, K.J. and Barreto, B. Use of DEM and elastic stability analysis to explain the influence of the intermediate principal stress on soil strength. *Géotechnique* (2013) **63**(15): 1298-1309.
[10] Tordesillas, A. and Muthuswamy, M. On the modeling of confined buckling of force chains. *J. Mech. Phys. Solids* (2009) **57**: 706–727.
[11] Hanley, K.J, O'Sullivan, C., Wadee, M.A. and Huang, X. Use of elastic stability analysis to explain the stress-dependent nature of soil strength. *Roy. Soc. Open Sci*. (2015) **2**: 150038.
[12] Huang, X., Hanley, K.J., O'Sullivan, C. and Kwok, C.Y. Exploring the influence of interparticle friction on critical state behavior using DEM. *Int. J. Num. Anal. Met*. (2014) **38**(12): 1276-1297.
[13] Peña, A.A., Lizcano, A., Alonso-Marroquin, F. and Herrmann, H.J. Biaxial test simulations using a packing of polygonal particles. *Int. J. Num. Anal. Met*. (2008) **32**(2): 143-160.
[14] Yang, Z.X., Yang, J. and Wang, L.Z. On the influence of inter-particle friction and dilatancy in granular materials: a numerical analysis. *Granul. Matter* (2012) **14**(3): 433-447.
[15] Smart, A.G. and Ottino, J.M. Evolving loop structure in gradually tilted two-dimensional granular packings. *Phys. Rev. E* (2008) **77**: 041307.
[16] Huang, X., Hanley, K.J., O'Sullivan, C. and Kwok, F.C.Y. Effect of sample size on the response of DEM samples with a realistic grading. *Particuology* (2014) **15**: 107-115.
[17] Simmons, G. and Brace, W.F. Comparison of static and dynamic measurements of compressibility of rocks. *J. Geophys. Res*. (1965) **70**: 5649-5656.
[18] Plimpton, S. Fast parallel algorithms for short-range molecular dynamics. *J. Comput. Phys*. (1995) **117**(1): 1-19.
[19] Thornton, C., Cummins, S.J. and Cleary, P.W. An investigation of the comparative behaviour of alternative contact force models during elastic collisions. *Powder Technol*. (2011) **210**(3): 189-197.
[20] Thornton, C., Cummins, S.J. and Cleary, P.W. An investigation of the comparative

behaviour of alternative contact force models during inelastic collisions. *Powder Technol*. (2013) **233**: 30-46.
[21] Yang, J. and Sze, H.Y. Cyclic behavior and resistance of saturated sand under non-symmetrical loading conditions. *Géotechnique* (2011) **61**(1): 59-73.
[22] Rycroft, C.H. Voro++: A three-dimensional Voronoi cell library in C++. *Chaos* (2009) **19**: 041111.
[23] The MathWorks Inc. MATLAB version 7.13 R2011b [computer software] (2011). Natick, Massachusetts, US.
[24] Horne, M.R. The behaviour of an assembly of rotund, rigid, cohesionless particles. III. *P. Roy. Soc. A-Math. Phy*. (1969) **310**(1500): 21-34.
[25] Caquot, A. *Équilibre des massifs à frottement interne: stabilité des terres, pulvérulentes ou cohérentes*. Gauthier-Villars, Paris (1934).
[26] Bishop, A.W. Discussion on 'Shear characteristics of a saturated silt, measured in triaxial compression'. *Géotechnique* (1954) **4**(1): 43-45.